

Prediction of the thermal entry length without solving the complete entrance length problem

Abraham J. Salazar

INTEVEP, S.A., Caracas, Venezuela

Antonio Campo

Mechanical Engineering Department, Florida International University, Miami, FL 33199, USA

A novel approximate solution has been devised for predicting the thermal entry length in duct flows for situations of either isothermal or isoflux walls and fully developed velocity distribution. The conventional partial differential energy equation does not need to be solved in the region of thermal development of the duct. This is a unique feature of the proposed solution, which has not been fully discussed in the literature before. Computed values of the thermal entry length for circular pipes and parallel plates are in good agreement with results obtained by more elaborate traditional techniques. These are the geometries most commonly used in fluid flow and heat transfer devices.

Keywords: convective heat transfer; duct flows; thermal entry length

Introduction

A reliable estimate of the magnitude of the thermal entry length in internal forced convection problems is very important to the heat-exchanger design engineer. This quantity establishes the borderline wherein heat transfer rates become dependent on or independent of the axial position of the duct. Beyond this point and under the idealization of laminar motion, the convective heat transfer coefficient depends on the fluid's thermal conductivity and the hydraulic diameter of the duct exclusively and is invariant with the axial coordinate.

The thermal entry length is traditionally defined as the duct length required to achieve a local value of Nu_x equal to 1.05 times the asymptotic value of the corresponding Nusselt number, Nu_{∞} , for a certain thermal boundary condition specified at the wall.¹ To arrive at this numerical value, the conventional procedure necessitates knowledge of the temperature field in the entire thermal entrance of the duct, obtained by solving the appropriate energy equation using analytical or numerical procedures. This information is converted into a local Nusselt number distribution, and the magnitude of the thermal entry length is eventually computed following the above-mentioned guidelines.

Conversely, Sandall and Hanna² devised a different approximate method to determine the thermal entry length for laminar flow through ducts exposed to uniform wall heat flux. Based on an overall energy balance between two consecutive cross sections of the duct, they derived an approximate value of $L_{th,\oplus}$. Comparison with the rigorous computation of $L_{th,\oplus}$ reported in Ref. 1 reveals that their expressions provide lower bounds for the exact value of $L_{th,\oplus}$. Computed errors are of the order of 15% and 33% for circular pipes and parallel plate channels, respectively. One drawback of the procedure developed in Ref. 2 is that its validity is restricted to an *a priori* knowledge of the

total wall heat flow passing to the fluid stream. Accordingly, the applicability of the method in Ref. 2 for practical problems is limited exclusively to situations involving an *a priori* knowledge of the wall heat fluxes.

On the other hand, although the development presented in Ref. 2 applied to a uniform heat flux boundary condition in a strict sense, Hanna *et al.* explored the possibility of extending their approximate approach for the case of uniform wall temperature.³ Accordingly, they stated that the essential difficulty with this thermal boundary condition is that the unknown surface heat flux, which varies with distance, is required for the analysis. In this regard, they estimated the magnitude of this heat flux by invoking a L ev eque-type solution with the understanding that it does not apply accurately over the whole thermal entrance region of the duct. In spite of this severe limitation, they proceeded with the original idea and their calculations supplied $L_{th,\oplus}^* = 0.0414$ for circular pipes. Of course, these values underpredicted the exact results of Shah,⁴ having associated errors of 38%. It should be noted that for case \oplus , Hanna *et al.*³ did not report results for the parallel plate geometrical configuration.

In a section devoted to areas of future research in Ref. 1, Shah and London recommended that improvements of the method proposed by Sandall and Hanna² be made without solving the complete entrance length problem. In addition, Shah and London suggested that the improved methodology be able to accommodate other thermal boundary conditions as well, characterizing a wide variety of heat exchange processes at the duct wall. In view of these arguments, we focused on a simplified approach to calculating the thermal entry length in duct flows, when subjected to any type of thermal boundary condition, without solving the complete entrance length problem. This approach is based on a combined analytical/numerical procedure that couples the classical method of separation of variables and the transversal method of lines. An extensive review of the latter was reported by Rothe.⁵ The salient feature of the procedure is that the temperature profile at any axial station $T(x, \zeta)$ in a duct can be calculated directly by solving a single ordinary differential equation (an equivalent energy

Address reprint requests to Professor Campo at the Department of Mechanical Engineering, Florida International University, Miami, FL 33199, USA.

Received 17 August 1988; accepted 1 August 1989

equation) at a preselected downstream position in the duct, instead of solving the complete partial differential equation (the energy equation), in the region of thermal development. Consequently, this ordinary differential equation, which incorporates the size of the axial station, emerges as a by-product of the proposed hybrid methodology identified by SETMOL (separation of variables/transversal method of lines). From here, calculation of the transverse temperature profile $T(\zeta)$ at any axial station is easily carried out numerically, and computation of the corresponding local Nusselt number is straightforward. Furthermore, specifying the calculated local Nusselt numbers at two or three distinct axial stations selected *a priori* allows a simple graphic interpolation to supply the approximate magnitude of the thermal entry length L_{th} . Two sample calculations for the limiting conditions of uniform wall temperature $\textcircled{1}$ and uniform wall heat flux $\textcircled{2}$ in circular pipes and parallel plate channels are included in this article to illustrate the simplicity of the proposed hybrid methodology.

Finally, it should be emphasized that this hybrid procedure is capable of handling any thermal boundary condition (linear). Additionally, work is underway to extend this procedure to ducts having any kind of irregular cross sections, which are commonly used in compact heat exchangers and nuclear reactors. Preliminary results are very encouraging.

Mathematical treatment

Under the assumption of fully developed velocity, the analysis will be presented for two cases: uniform wall temperature $\textcircled{1}$ and uniform wall heat flux $\textcircled{2}$.

Uniform wall temperature $\textcircled{1}$

The dimensionless transverse temperature in a duct is governed by the ordinary differential equation

$$\frac{1}{\eta^c} \frac{d}{d\eta} \left(\eta^c \frac{d\theta}{d\eta} \right) = \frac{1}{\Delta X} \left(\frac{L_c}{D_h} \right) U \theta \ln|\theta| \quad (1)$$

where $\theta(\eta)$ designates the temperature variation at a distance ΔX from the origin. Step-by-step details of this derivation appear in Appendix A. Furthermore, Equation 1 is subject to the boundary conditions

$$\frac{d\theta}{d\eta} = 0, \quad \eta = 0 \quad (2)$$

and

$$\theta = 0, \quad \eta = 1 \quad (3)$$

Uniform wall heat flux $\textcircled{2}$

The conventionally adopted superposition principle allows us to write the dimensionless temperature field in two parts, namely,

$$\Theta = \varphi + \Theta_{fd} \quad (4)$$

where

$$\Theta_{fd} = 4X + \eta^2 - \frac{\eta^4}{4} - \frac{14}{48} \quad (5)$$

designates the fully developed temperature profile for a circular tube and

$$\Theta_{fd} = 4X + \frac{3}{4} \eta^2 - \frac{\eta^4}{8} - \frac{39}{280} \quad (6)$$

is the corresponding fully developed temperature profile for a parallel plate channel. Hence the developing temperature profile in the transverse direction $\varphi(\eta)$ at a distance ΔX from the origin is characterized by the ordinary differential equation

$$\frac{1}{\eta^c} \frac{d}{d\eta} \left(\eta^c \frac{d\varphi}{d\eta} \right) = \frac{1}{\Delta X} \left(\frac{L_c}{D_h} \right) U \varphi \ln \left(\frac{|\varphi|}{|\Theta_{01}|} \right) \quad (7)$$

where by virtue of the boundary condition at the entrance $X=0$,

$$\Theta_0 = -\Theta_{fd}(0, \eta) \quad (8)$$

Again, this derivation is explained in Appendix A.

Notation

c	Geometric parameter ($c=1$ for pipes; $c=0$ for parallel plates)
D	Pipe diameter
D_h	Hydraulic diameter ($D_h=D$ for pipes; $D_h=4L$ for parallel plates)
h	Convection coefficient
k	Thermal conductivity
L	Half-spacing of parallel plates
L_c	Characteristic length ($L_c=R$ for pipes; $L_c=L$ for parallel plates)
L_{th}	Thermal entry length
L_{th}^*	Dimensionless thermal entry length, $L_{th}/L_c Pe$
Nu_m	Mean Nusselt number, $h_m D_h/k$
Nu_x	Local Nusselt number, $h_x D_h/k$
Nu_∞	Asymptotic Nusselt number
Pe	Peclet number, $u_m D_h/\alpha$
q_w	Wall heat flux
r	Transverse coordinate for pipes
R	Pipe radius
T	Temperature
u	Fully developed velocity
U	Dimensionless velocity, u/u_m
x	Axial coordinate

X	Dimensionless axial coordinate, $x/L_c Pe$
y	Transverse coordinate for parallel plates

Greek letters

α	Thermal diffusivity
ΔX	Axial station
ζ	Generalized transverse coordinate ($\zeta=r$ for pipes; $\zeta=y$ for parallel plates)
η	Dimensionless value of ζ , ζ/L_c
θ	Dimensionless temperature for case $\textcircled{1}$, $(T-T_w)/(T_c-T_w)$
Θ	Dimensionless temperature for case $\textcircled{2}$, $k(T-T_c)/q_w L_c$
φ	Dimensionless temperature for case $\textcircled{2}$, Equation 4
ψ	Generalized dimensionless temperature, Equation 11

Subscripts

b	Mean bulk
e	Inlet
fd	Fully developed
$\textcircled{2}$	Refers to uniform wall heat flux
m	Mean
$\textcircled{1}$	Refers to uniform wall temperature
w	Wall
x	Local value

In addition, by invoking Equation 4, we may write the boundary conditions associated with Equation 7 as

$$\frac{d\varphi}{d\eta} = 0, \quad \eta = 0 \tag{9}$$

and

$$\frac{d\varphi}{d\eta} = 0, \quad \eta = 1 \tag{10}$$

respectively.

Note that Equations 1–3 and 7–10 constitute a boundary value problem, and its solution does not require a marching technique. Consequently, the transverse temperature profiles may be readily computed at any axial station ΔX by solving the corresponding system of algebraic equations at each ΔX .

Conversely, knowledge of the fluid's temperature profile is the only necessary ingredient for the calculation of the mean bulk temperature $\psi_b(\Delta X)$ at any axial station ΔX :

$$\psi_b = 4 \left(\frac{L_c}{D_h} \right) \int_0^1 U \psi \eta^2 d\eta \tag{11}$$

where ψ designates a generalized temperature; $\psi = \theta$ for case $\textcircled{1}$, and $\psi = \Theta$ for case $\textcircled{2}$, respectively.

As stated in the Introduction, the magnitude of the thermal entry length is influenced by the asymptotic values of the local Nusselt number Nu_∞ in the downstream region of the duct. Accordingly, these local Nusselt numbers for cases $\textcircled{1}$ and $\textcircled{2}$ are expressed by

$$Nu_x = \frac{\left(\frac{d\theta}{d\eta} \right)_w}{\left(\frac{L_c}{D_h} \right) \theta_b} \tag{12}$$

and

$$Nu_x = \frac{1}{\left(\frac{L_c}{D_h} \right) (\Theta_w - \Theta_b)} \tag{13}$$

respectively. This information leads to the direct calculation of the thermal entry length L_{th} , which is somewhat arbitrarily defined in Ref. 1 as the duct length wherein $Nu_x = 1.05 Nu_\infty$. Additionally, the mean Nusselt number for case $\textcircled{1}$ is given by the relation

$$Nu_m = \frac{1}{4X \left(\frac{L_c}{D_h} \right)} \ln \left(\frac{1}{\theta_b} \right) \tag{14}$$

Numerical procedure

Since the source term in Equations 1 and 7 depends on both position and temperature, standard analytical methods do not exist, and a numerical approach capable of handling nonlinear terms is mandatory. Correspondingly, the most elementary of these approaches involves the solution of a system of linear algebraic equations by the Gauss–Seidel technique and updating the nonlinear source term between two consecutive iterations.

However, in this article results have been obtained by employing a readily available subroutine, based on a finite-difference procedure called PASVA3, developed by Pereyra.⁶ In this method, each transformed ordinary differential equation, i.e., Equations 1 and 7, are rewritten in finite differences at

certain preselected stations ΔX (see Figure 1). The resulting systems of nonlinear algebraic equations are solved iteratively until convergence is achieved. For these particular problems, the nodal points are clustered closer to the duct wall in order to resolve the larger temperature gradients that occur near it. The grid point distribution is carefully tailored to yield transverse temperature profiles that are grid-independent at any axial station ΔX in the downstream region of the duct.

Results and discussion

In the present study, quantitative information on the thermal entry length has been obtained for two limiting cases within the framework of thermal boundary conditions, namely, $\textcircled{1}$ and $\textcircled{2}$. Typical results are given below for two geometrically extreme cases: circular pipe and parallel plate channel.

Circular pipe

Case $\textcircled{2}$. By solving Equation 7 at three different stations, e.g., $\Delta X = 0.04, 0.06,$ and $0.1,$ we can readily determine the corresponding radial temperature profiles $\Theta(\eta)$ and the local Nusselt numbers Nu_x . This information may be plotted on semilog paper, as illustrated in Figure 2. Graphic interpolation between these three points reveals that the approximate thermal entry length $L_{th,\textcircled{2}}$ is 0.0868. Judging from the crude analysis based on SETMOL proposed here, this quantity compares extremely well with the benchmark solution for the entire thermal entrance length problem reported in Shah,⁴ wherein $L_{th,\textcircled{2}} = 0.0861$. If more accurate results are necessary, an improved estimate of $L_{th,\textcircled{2}}$ may be obtained for interpolation purposes by reducing the intervals of ΔX to subintervals in the neighborhood of $X = 0.0868,$ as shown in the inset of Figure 2 (see Appendix B). Furthermore, the estimate of $L_{th,\textcircled{2}}$ provided by Sandall and Hanna² was 0.0730.

Case $\textcircled{1}$. For this thermal boundary condition, implementation of the procedure explained for case $\textcircled{2}$ is a bit more elaborate. Basically, this is due to the fact that the wall temperature gradient $(d\theta/d\eta)_w,$ which is directly proportional to $Nu_x,$ is not a fixed quantity as it was in case $\textcircled{2},$ and therefore needs to be calculated. Correspondingly, it has been clearly stated that the adopted hybrid methodology SETMOL provides an *approximate* temperature profile at any downstream axial station. Consequently, minor temperature deviations usually yield significant errors when the important quantity—the local wall temperature gradient—needs to be computed accurately.

An alternative route that circumvents this inherent difficulty will be developed in this section. Accordingly, the descriptive ordinary differential equation, Equation 1, must be solved at a minimum of two axial stations. Next, the mean Nusselt number Nu_m at each of the participating stations may be obtained from Equation 14.

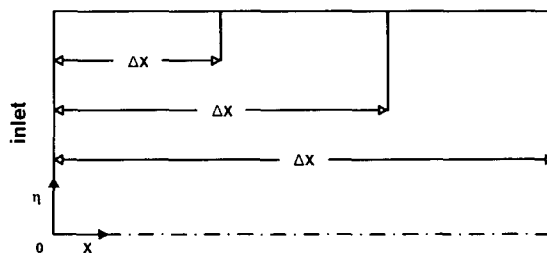


Figure 1 Preselected stations where temperature profiles are desired

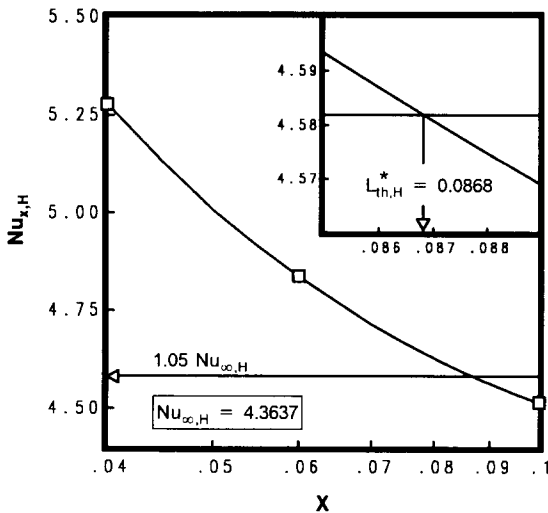


Figure 2 Variation of Nu_x in a circular pipe, case (H)

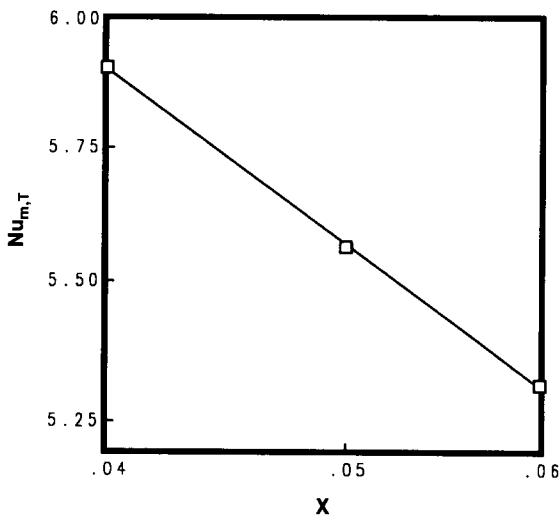


Figure 3 Variation of Nu_m in a circular pipe, case (T)

obtained from Equation 14.

On the other hand, exploiting the linear behavior of $\log Nu_m$ versus $\log X$, we may write

$$\ln Nu_m = a + b \ln X \tag{15a}$$

which, in turn, becomes

$$Nu_m = e^a X^b \tag{15b}$$

Alternatively, by definition, the relationship between Nu_x and Nu_m may be expressed as follows:

$$Nu_x = Nu_m + X \left(\frac{dNu_m}{dX} \right) \tag{16}$$

Furthermore, inserting Equation 15b into Equation 16 results in the relation

$$Nu_m = \frac{Nu_x}{1+b} \tag{17}$$

Additionally, equating Equations 15b and 17 yields

$$\frac{Nu_x}{1+b} = e^a X^b \tag{18}$$

Inspection of Equation 18 reveals a power-law type of variation for the distribution of the local Nusselt number Nu_x . Hence, invoking the criterion for the thermal entry length (Ref. 1) and consequently replacing X by $L_{th,\oplus}^*$ and Nu_x by $1.05Nu_\infty$ in Equation 18, respectively, leads to the compact expression

$$L_{th,\oplus}^* = \left[\frac{1.05Nu_\infty}{(1+b)e^a} \right]^{1/b} \tag{19}$$

An interesting feature of the adopted methodology as applied to case (T) is that Equation 19 allows for a direct calculation of $L_{th,\oplus}^*$. The reason is that Nu_∞ is a known quantity, and a and b are just constants corresponding to the intercept and the slope of the Nu_m curve, respectively, i.e., Equation 15a.

A sample calculation will be discussed briefly. Figure 3 shows the linear log-log variation of Nu_m versus X . This plot results from the evaluation of Equation 15a based on the computation of the temperature profiles at three distinct stations: $X=0.04$, 0.05 , and 0.06 . The constants $a=0.9377$ and $b=-0.2602$ are readily determined graphically or, more accurately, by implementing a least squares curve-fitting technique. Introducing these numbers, along with $Nu_{\infty,T}=3.6568$, into Equation 19 gives $L_{th,\oplus}^*=0.06554$. Meanwhile, the analytically determined value reported by Shah is $L_{th,\oplus}^*=0.06693$. Figure 4 further illustrates the variation of Nu_x as calculated from Equation 18. Conventional interpolation confirms the value of $L_{th,\oplus}^*$ as 0.0655 . There appears to be good qualitative agreement between this approximate solution and Shah's exact solution. It should also be mentioned that the computed value of $L_{th,\oplus}^*$, using the L ev eque solution reported in Ref. 3, was 0.0414 .

Parallel plate channel

Case (T). As with the circular duct, upon solving Equation 7 at three different stations, e.g. $\Delta X=0.02$, 0.04 , and 0.08 , the corresponding transverse temperature profiles $\Theta(\eta)$ and the associated local Nusselt numbers Nu_x are readily determined. Next, this information is plotted on semilog paper, as illustrated in Figure 5. Graphic interpolation between these three points clearly reveals that the approximate value of the thermal entry

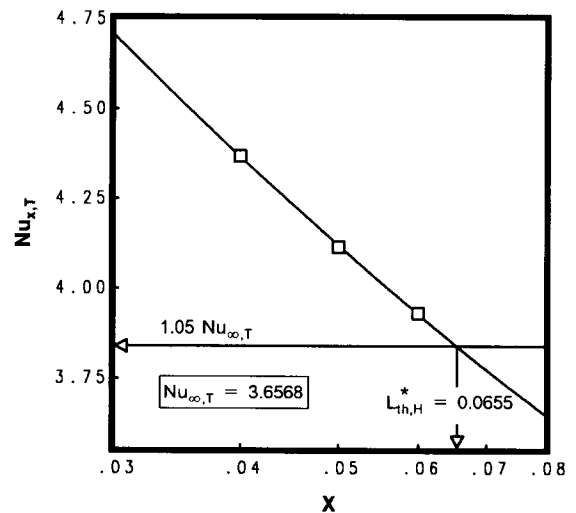


Figure 4 Variation of Nu_x in a circular pipe, case (T)

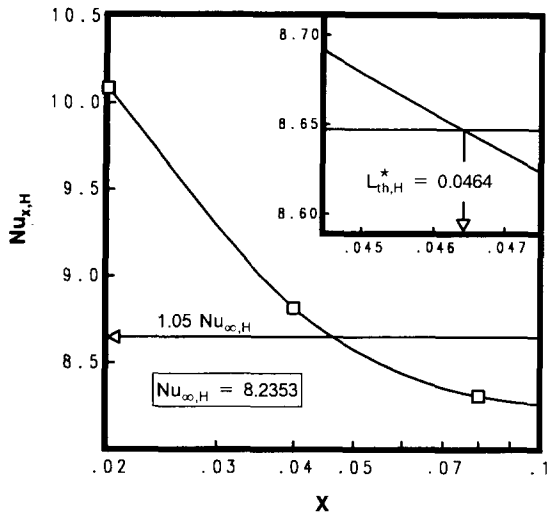


Figure 5 Variation of Nu_x in a parallel plate channel, case (H)

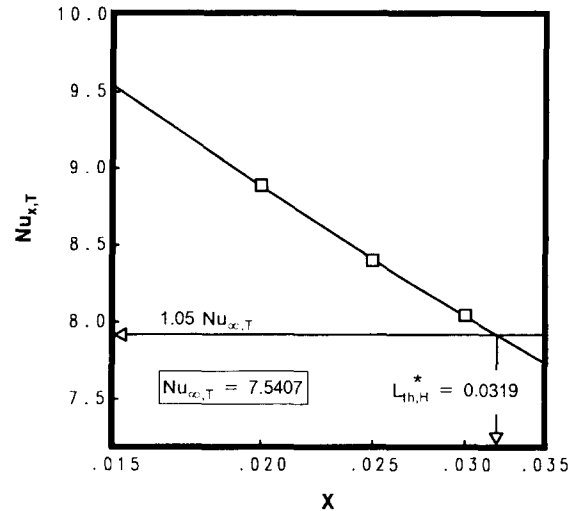


Figure 7 Variation of Nu_x in a parallel plate channel, case (T)

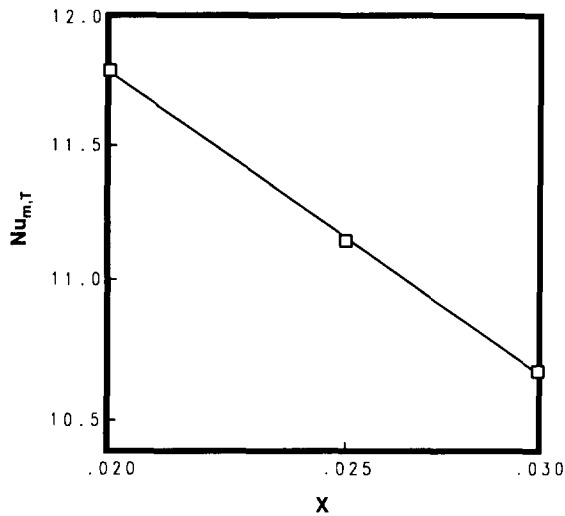


Figure 6 Variation of Nu_m in a parallel plate channel, case (T)

length $L_{th,\textcircled{H}}^*$ is 0.0464. Therefore, as in the circular pipe, this quantity compares extremely well with Shah's benchmark solution⁴ of the entire thermal entrance problem, wherein $L_{th,\textcircled{H}}^* = 0.0462$. As mentioned before, more accurate results may be obtained by reducing the intervals of ΔX to subintervals in the neighborhood of $X = 0.0464$, as shown in the inset of Figure 5 (see Appendix B). On the other hand, the procedure developed in Ref. 2 yielded a value of $L_{th,\textcircled{H}}^* = 0.0348$.

Case (T). By repeating the step-by-step procedure employed for the circular duct configuration, the temperature profiles are computed at three stations, i.e., $X = 0.02, 0.025$, and 0.03 , and Nu_m is evaluated. Figure 6 shows the local linear variation of $\log Nu_m$ with $\log X$. Based on this variation, the numerical values of a and b may be readily computed; i.e., $a = 1.5037$ and $b = -0.2462$, respectively.

Moreover, introducing a and b , along with $Nu_{\infty,\textcircled{T}} = 7.541$ into Equation 19 gives $L_{th,\textcircled{T}}^* = 0.0319$. This quantity agrees well with the analytically determined value of $L_{th,\textcircled{T}}^* = 0.0319$, reported by Shah. For completeness, Figure 7 depicts the variation of Nu_x , as calculated from Equation 18.

Conclusions

This paper is concerned with an approximate calculation of the thermal entry length in laminar forced convection flows through regular ducts without solving the governing energy equation. The solution methodology, based on the method of separation of variables and the transversal method of lines (SETMOL), is especially useful for practitioners in heat exchanger applications. Step-by-step calculations were demonstrated for two limiting thermal boundary conditions, (T) and (H), in conjunction with two extreme geometric configurations (circular pipe and parallel plate channel). It was found that in all cases the computed thermal entry lengths were within 2% of the corresponding lengths obtained from benchmark analytical solutions reported by Shah.⁴ His work corresponds to the complete solution of the thermal entrance problem. Conversely, the predictions reported in Refs. 2 and 3 were found to be less accurate than those of the present investigation.

The excellence of these predictions establishes the present methodology as a viable tool for computing the thermal entry length in duct flow heat transfer problems. Work is currently underway to extend this theory for predicting the thermal entry length of ducts of irregular cross sections normally used in compact heat exchangers.

References

- 1 Shah, R. K. and London, A. L. *Laminar Flow Forced Convection in Ducts*. Academic Press, New York, 1978
- 2 Sandall, O. C. and Hanna, O. T. Entrance lengths for transport with a specified surface flux. *AIChE J.* 1973, **19**, 867-870
- 3 Hanna, O. T., Sandall, O. C., and Paruit, B. A. Thermal entrance lengths for laminar flow in various ducts for constant surface heat flux. *Trans. Heat Mass Transf.* 1976, **3**, 89-97
- 4 Shah, R. K. Thermal entry length solutions for the circular tube and parallel plates. Paper No. HMT-11-75, presented at the 1975 National Heat and Mass Transfer Conference, Bombay
- 5 Rothe, E. Zweidimensionale parabolische Randwertaufgaben als Grenzfall eindimensionaler Randwertaufgaben. *Math. Ann.* 1930, **102**, 650-670
- 6 Pereyra, V. PASVA3: An adaptive finite difference FORTRAN program for first order nonlinear ordinary boundary problems. *Lecture Notes in Computer Sciences*, **76**, 67-78, Springer-Verlag, Berlin, 1978

Appendix A

Mathematical derivation of eq. (1)

In terms of a generalized variable Λ , the applicable energy equation in dimensionless form is given by

$$\left(\frac{L_c}{D_h}\right)U \frac{\partial \Lambda}{\partial X} = \frac{1}{\eta^c} \frac{\partial}{\partial \eta} \left(\eta^c \frac{\partial \Lambda}{\partial \eta} \right) \quad (A-1)$$

where c designates a geometric parameter.

Invoking the method of separation of variables allows assumptions of a series solution of Equation A-1 as follows:

$$\Lambda = \sum_{i=0}^{\infty} a_i Z_i(X) Y_i(\eta) \quad (A-2)$$

where Z_i are functions of X only, Y_i are functions of η only, and a_i are coefficients.

Combining Equations A-1 and A-2 yields

$$\sum_{i=0}^{\infty} a_i \left[\left(\frac{L_c}{D_h}\right)U Z_i' Y_i - Z_i Y_i'' - \frac{c}{\eta^c} Z_i Y_i' \right] = 0 \quad (A-3)$$

Because the coefficients a_i are arbitrary, Equation A-3 is satisfied when the terms in brackets are

$$\left(\frac{L_c}{D_h}\right)U Z_i' Y_i - Z_i Y_i'' - \frac{c}{\eta^c} Z_i Y_i' = 0 \quad (A-4)$$

Next, separating variables in Equation A-4 results in the following set of ordinary differential equations:

$$Z_i' + \lambda_i^2 Z_i = 0 \quad (A-5)$$

$$Y_i'' + \frac{c}{\eta} Y_i' + \lambda_i^2 \left(\frac{L_c}{D_h}\right)U Y_i = 0 \quad (A-6)$$

where λ_i are the corresponding eigenvalues. Now, multiplying Equations A-5 and A-6 by Y_i and Z_i , respectively, and performing the summation on the i index, gives

$$\frac{\partial \Lambda}{\partial X} = - \sum_{i=0}^{\infty} a_i \lambda_i^2 Z_i Y_i \quad (A-7)$$

and

$$\frac{\partial^2 \Lambda}{\partial \eta^2} + \frac{c}{\eta} \frac{\partial \Lambda}{\partial \eta} = - \left(\frac{L_c}{D_h}\right)U \sum_{i=0}^{\infty} a_i \lambda_i^2 Z_i Y_i \quad (A-8)$$

At this stage, a function $\bar{\lambda}^2(X, \eta)$ is defined by

$$\bar{\lambda}^2 = \bar{\lambda}^2(X, \eta) = \frac{\sum_{i=0}^{\infty} a_i \lambda_i^2 Z_i Y_i}{\sum_{i=0}^{\infty} a_i Z_i Y_i} \quad (A-9)$$

From a conceptual point of view, this function may be interpreted as a weighted average value of the squares of the eigenvalues λ_i .

Next, introducing this definition into Equations A-7 and A-8 leads to the system

$$\frac{\partial \Lambda}{\partial X} = - \bar{\lambda}^2 \Lambda \quad (A-10)$$

and

$$\frac{\partial^2 \Lambda}{\partial \eta^2} + \frac{c}{\eta} \frac{\partial \Lambda}{\partial \eta} = - \left(\frac{L_c}{D_h}\right)U \bar{\lambda}^2 \Lambda \quad (A-11)$$

Despite the fact that $\bar{\lambda}^2 = \bar{\lambda}^2(X, \eta)$ appears in the preceding equations, its actual use for the computation of Λ at $X = \Delta X$ requires that we realize that $\bar{\lambda}^2 = \bar{\lambda}^2(\Delta X, \eta)$. In other words, $\bar{\lambda}^2$ becomes a function of η only, because it has been evaluated at a fixed axial station ΔX . Therefore we may safely assume that $\bar{\lambda}^2$ is an independent function of X . Hence, carrying out the integration of Equation A-10 results in

$$\Lambda = C_0(\eta) e^{-\bar{\lambda}^2 X} \quad (A-12a)$$

where $C_0(\eta)$ may be evaluated from the boundary condition at $X=0$, namely,

$$\Lambda_0 = \Lambda(X=0) = C_0(\eta) \quad (A-12b)$$

Then we can write $\bar{\lambda}^2$ explicitly as a function of Λ :

$$\bar{\lambda}^2 = -X^{-1} \ln \left(\frac{|\Lambda|}{|\Lambda_0|} \right) \quad (A-13)$$

Conversely, we may now turn our attention to Equation A-11. Introducing Equation A-13 into Equation A-11 gives

$$\frac{\partial^2 \Lambda}{\partial \eta^2} + \frac{c}{\eta} \frac{\partial \Lambda}{\partial \eta} - \left(\frac{L_c}{D_h}\right) \frac{U}{X} \ln \left(\frac{|\Lambda|}{|\Lambda_0|} \right) \Lambda = 0 \quad (A-14)$$

Then let ΔX designate an interval between the entrance $X=0$ and any axial station $X=X$ placed in the downstream portion of the channel (see Figure 1). Therefore, by virtue of the transversal method of lines,⁵ Equation A-14 becomes

$$\frac{d^2 \Lambda}{d\eta^2} + \frac{c}{\eta} \frac{d\Lambda}{d\eta} - \left(\frac{L_c}{D_h}\right) \frac{U}{\Delta X} \ln \left(\frac{|\Lambda|}{|\Lambda_0|} \right) \Lambda = 0 \quad (A-15)$$

Mathematically, Equation A-15 constitutes a transformed equation of energy conservation, where $\Lambda(\eta)$ designates a radial profile at any particular station, ΔX , in the downstream region of thermal development in the channel. Thus, Equation A-15 indeed constitutes a two-point boundary value problem given by a nonlinear ordinary differential equation that results from the combination of the method of separation of variables and the transversal method of lines (SETMOL).

Appendix B

Possible improvement

Once the approximate value of L_{th}^* is determined for any geometry and any thermal boundary condition, a refined estimate of it may be obtained as follows. The necessary number of axial stations for each case tested may be assigned in the neighborhood of the first estimate of L_{th}^* , and the process is repeated in an appropriate set of subintervals of the axial dimensionless coordinate X . This step-by-step process is repeated until good convergence is achieved.